

I. SOME LAGRANGE INTERPOLATION FUNCTIONS FOR SOLENOIDAL AND IRROTATIONAL VECTOR FIELDS

JONAS T. HOLDEMAN

Dedicated to Louis B. Holdeman & Edward G. Miller, fallen friends. Our ranks thin. March on!

ABSTRACT. Some remarkable new Lagrange interpolation functions on rectangular Cartesian meshes in two dimensions, and rectangular hexahedral meshes in three dimensions, are developed. The first examples are linearly-complete with a common (constant) divergence or a common (constant) curl on each element or subdomain of the mesh. These are extended to quadratic-complete functions, and then extended to orthogonal curvilinear coordinate systems, and affine meshes in those systems. After revisiting the equation of motion for incompressible flow, the functions, with suitable constraints, are used with the finite element method (FEM) to solve the incompressible Stokes equation.

1. INTRODUCTION

It is perhaps surprising how limited the class of interpolation functions for interpolating solenoidal or irrotational fields while preserving the solenoidal or irrotational properties in a strong or pointwise sense is, and how elusive the search for better functions has been, particularly in three dimensions. The goal would be to find functions which are sufficiently continuous to be completely divergence- or curl-free. The latter could be satisfied by taking the curl or gradient of a “potential” function, but the class of recognized potential functions with sufficient continuity has been very small. Ultimately, the solution lies in the class of Hermite interpolation functions with the span of the curl in the space of functions $\mathbf{H}(\text{div}, \Omega)$, square-integrable with square-integrable curl over the domain Ω , or with the span of the gradient in the space of functions $\mathbf{H}(\text{curl}, \Omega)$, square-integrable with square-integrable gradient. As a first step toward this goal, we demonstrate sufficiently continuous Lagrange interpolation functions with the properties that their divergences or curls have a common functional form. Then with a linear constraint, the sum of the contributions from the various nodes can be made to cancel. The Lagrange interpolation functions to be described are very useful in their own right, but they are also the basis for developing the Hermite functions to be described in a later paper [6].

The unqualified use of the term “divergence-free” in this paper means strongly or pointwise divergence-free in the problem domain, including the interfaces between the subdomains or elements. This is in contrast to “weakly divergence-free,”

Prepared January 24, 2003.

2000 *Mathematics Subject Classification.* Primary 65D05; Secondary 65N30, 76D05.

commonly used without qualification, which means divergence-free in a (weighted) average sense, and to certain non-conforming piecewise interpolations.

In the context of the incompressible Navier-Stokes equation, a number of different forms are used which are formally, but not computationally identical in the weak case. The strongly solenoidal properties of the Lagrange functions presented here make these forms computationally indistinguishable, provided a rather trivial form of the continuity constraint is satisfied.

2. LINEAR FUNCTIONS ON ORTHOGONAL CARTESIAN MESHES

The starting points here are the classical bilinear and trilinear interpolation functions. Consider a typical element or subdomain of the mesh, a rectangular hexahedron with dimensions $\{h_x, h_y, h_z\}$ and center (x_c, y_c, z_c) , and with indices $\hat{x}_i, \hat{y}_i, \hat{z}_i = \pm 1$ or 0. For simplicity and economy of display, we give the forms in terms of dimensionless or normalized variables with some dimensional constants,

$$(2.1) \quad \begin{aligned} \xi &\equiv \frac{2}{h_x}(x - x_c), & \xi_0 &\equiv \hat{x}_i \xi, & \xi_h &\equiv \frac{2}{h_x}, & \xi_i &\equiv \hat{x}_i \xi_h, \\ \eta &\equiv \frac{2}{h_y}(y - y_c), & \eta_0 &\equiv \hat{y}_i \eta, & \eta_h &\equiv \frac{2}{h_y}, & \eta_i &\equiv \hat{y}_i \eta_h, \\ \zeta &\equiv \frac{2}{h_z}(z - z_c), & \zeta_0 &\equiv \hat{z}_i \zeta, & \zeta_h &\equiv \frac{2}{h_z}, & \zeta_i &\equiv \hat{z}_i \zeta_h. \end{aligned}$$

First, consider the two-dimensional case. The interpolated vector field on the typical element e is given by,

$$(2.2) \quad \mathbf{V}^e = \sum_{i \in e} \mathbf{N}_i(\xi, \eta) \begin{bmatrix} u_i \\ v_i \end{bmatrix},$$

where the sum is over the mesh nodes i involving the element. The four-node bilinear interpolation function for a two-dimensional vector field is,

$$(2.3) \quad \mathbf{N}_i(\xi, \eta) = \mathbf{N}_i^{4B}(\xi, \eta) = \begin{bmatrix} \frac{1}{4}(1 + \xi_0)(1 + \eta_0) & 0 \\ 0 & \frac{1}{4}(1 + \xi_0)(1 + \eta_0) \end{bmatrix}.$$

One can find bilinear-based functions with a common-divergence (CD) (or consistent-divergence) which is constant by finding off-diagonal functions such that the divergence of the columns is constant,

$$(2.4) \quad \mathbf{N}_i^{4D}(\xi, \eta) = \begin{bmatrix} \frac{1}{4}(1 + \xi_0)(1 + \eta_0) & \frac{1}{8}\eta_i \xi_i^{-1}(1 - \xi^2) \\ \frac{1}{8}\xi_i \eta_i^{-1}(1 - \eta^2) & \frac{1}{4}(1 + \xi_0)(1 + \eta_0) \end{bmatrix}.$$

Likewise, one can find common (consistent) curl (CC) functions such that the curl of the columns is constant,

$$(2.5) \quad \mathbf{N}_i^{4C}(\xi, \eta) = \begin{bmatrix} \frac{1}{4}(1 + \xi_0)(1 + \eta_0) & -\frac{1}{8}\xi_i \eta_i^{-1}(1 - \eta^2) \\ -\frac{1}{8}\eta_i \xi_i^{-1}(1 - \xi^2) & \frac{1}{4}(1 + \xi_0)(1 + \eta_0) \end{bmatrix}.$$

In three dimensions, the eight-node trilinear-based constant-divergence interpolation function is,

$$(2.6) \quad \mathbf{N}_i^{8D}(\xi, \eta, \zeta) = \begin{bmatrix} \frac{1}{8}(1 + \xi_0)(1 + \eta_0)(1 + \zeta_0) & \frac{1}{32}\eta_i \xi_i^{-1}(1 - \xi^2)(2 + \zeta_0) & \frac{1}{32}\zeta_i \xi_i^{-1}(1 - \xi^2)(2 + \eta_0) \\ \frac{1}{32}\xi_i \eta_i^{-1}(1 - \eta^2)(2 + \xi_0) & \frac{1}{8}(1 + \xi_0)(1 + \eta_0)(1 + \zeta_0) & \frac{1}{32}\zeta_i \eta_i^{-1}(1 - \eta^2)(2 + \xi_0) \\ \frac{1}{32}\xi_i \zeta_i^{-1}(1 - \zeta^2)(2 + \eta_0) & \frac{1}{32}\eta_i \zeta_i^{-1}(1 - \zeta^2)(2 + \xi_0) & \frac{1}{8}(1 + \xi_0)(1 + \eta_0)(1 + \zeta_0) \end{bmatrix},$$

But there is no trilinear-based *constant-curl* Lagrange interpolation function. This lack is of little consequence for irrotational interpolation, as there is an elegant resolution in terms of Hermite interpolation functions which will be presented in a later paper [6].

These functions are “linearly-complete” over their respective fields, a property which will be essential in a section to follow. In addition to the constant field, these functions interpolate all linear fields which are solenoidal or irrotational, as the case may be. However, for a given corner node, these functions do not completely vanish on non-adjacent sides or faces. While the *constant-divergence* functions are continuous in the normal directions at those sides and faces, the tangential component does not vanish. This is of no consequence as far as the divergence is concerned, as only normal derivatives need be continuous. The space spanned by these functions lies in the space $\mathbf{H}(\text{div}, \Omega)$. Similarly, the *constant-curl* and linear-curl functions are tangentially-, but not normally-continuous and interpolants lie in $\mathbf{H}(\text{curl}, \Omega)$. These are, in fact, only potential discontinuities. Since the unisolvence sets of these functions are linearly complete, the interpolations of linear fields are necessarily continuous.

3. QUADRATIC FUNCTIONS ON RECTILINEAR CARTESIAN MESHES

Quadratic-complete interpolation functions are found by introducing functions associated with nodes on the mid-sides of the edges. Only the normal vector components need be considered for the CD functions. This should not be surprising as the other tangential components are not under control by the corner nodes. Using the matrix representation again, off-diagonal functions are found such that the divergence of the columns is constant. Then subtracting one-half of these functions from the linear corner functions so that the normal components of the new corner functions vanish at the edge nodes, one finds

$$(3.1) \quad \mathbf{N}_i^{\text{8D}}(\xi, \eta) = \begin{cases} \begin{bmatrix} \frac{1}{4}(1 + \xi_0)(1 + \eta_0)\eta_0 & \frac{1}{8}\eta_i\xi_i^{-1}(1 - \xi^2)(1 + \frac{2}{3}\xi_0) \\ \frac{1}{8}\xi_i\eta_i^{-1}(1 - \eta^2)(1 + \frac{2}{3}\eta_0) & \frac{1}{4}(1 + \xi_0)(1 + \eta_0)\xi_0 \end{bmatrix} & \begin{matrix} \xi_i = \pm 1, \\ \eta_i = \pm 1, \end{matrix} \\ \begin{bmatrix} \frac{1}{2}(1 + \xi_0)(1 - \eta^2) & 0 \\ -\frac{1}{6}\xi_i\eta_h^{-1}\eta(1 - \eta^2) & 0 \end{bmatrix} & \begin{matrix} \xi_i = \pm 1, \\ \eta_i = 0, \end{matrix} \\ \begin{bmatrix} 0 & -\frac{1}{6}\eta_i\xi_h^{-1}\xi(1 - \xi^2) \\ 0 & \frac{1}{2}(1 + \eta_0)(1 - \xi^2) \end{bmatrix} & \begin{matrix} \xi_i = 0, \\ \eta_i = \pm 1. \end{matrix} \end{cases}$$

Proceeding in the same manner for the constant-curl case gives,

$$(3.2) \quad \mathbf{N}_i^{\text{8C}}(\xi, \eta) = \begin{cases} \begin{bmatrix} \frac{1}{4}(1 + \xi_0)(1 + \eta_0)\xi_0 & -\frac{1}{8}\xi_i\eta_i^{-1}(1 - \eta^2)(1 + \frac{2}{3}\eta_0) \\ -\frac{1}{8}\eta_i\xi_i^{-1}(1 - \xi^2)(1 + \frac{2}{3}\xi_0) & \frac{1}{4}(1 + \xi_0)(1 + \eta_0)\eta_0 \end{bmatrix} & \begin{matrix} \xi_i = \pm 1, \\ \eta_i = \pm 1, \end{matrix} \\ \begin{bmatrix} \frac{1}{2}(1 + \eta_0)(1 - \xi^2) & 0 \\ \frac{1}{6}\eta_i\xi_h^{-1}\xi(1 - \xi^2) & 0 \end{bmatrix} & \begin{matrix} \xi_i = 0, \\ \eta_i = \pm 1, \end{matrix} \\ \begin{bmatrix} 0 & \frac{1}{6}\xi_i\eta_h^{-1}\eta(1 - \eta^2) \\ 0 & \frac{1}{2}(1 + \xi_0)(1 - \eta^2) \end{bmatrix} & \begin{matrix} \xi_i = \pm 1, \\ \eta_i = 0. \end{matrix} \end{cases}$$

Likewise, for constant-divergence interpolation in three-dimensions one finds the 20-node functions,

$$(3.3) \quad \mathbf{N}_i^{20D}(x, y, z) = \begin{bmatrix} \frac{1}{8}(1 + \xi_0)(1 + \eta_0) \\ (1 + \zeta_0)(\eta_0 + \zeta_0 - 1) \\ \frac{1}{96}\xi_i\eta_i^{-1}(1 - \eta^2) \\ (1 + 3\zeta_0 + 3\zeta^2 + 2\eta_0(2 + \zeta_0)) \\ \frac{1}{96}\xi_i\zeta_i^{-1}(1 - \zeta^2) \\ (1 + 3\eta_0 + 3\eta^2 + 2\zeta_0(2 + \eta_0)) \end{bmatrix}$$

$$\left. \begin{array}{l} \frac{1}{96}\eta_i\xi_i^{-1}(1 - \xi^2) \\ (1 + 3\zeta_0 + 3\zeta^2 + 2\xi_0(2 + \zeta_0)) \\ \frac{1}{8}(1 + \xi_0)(1 + \eta_0) \\ (1 + \zeta_0)(\xi_0 + \zeta_0 - 1) \\ \frac{1}{96}\eta_i\zeta_i^{-1}(1 - \zeta^2) \\ (1 + 3\xi_0 + 3\xi^2 + 2\zeta_0(2 + \xi_0)) \end{array} \right\} \begin{array}{l} \hat{x}_i = \pm 1, \\ \hat{y}_i = \pm 1, \\ \hat{z}_i = \pm 1, \end{array}$$

$$\left. \begin{array}{l} \frac{1}{96}\zeta_i\xi_i^{-1}(1 - \xi^2) \\ (1 + 3\eta_0 + 3\eta^2 + 2\xi_0(2 + \eta_0)) \\ \frac{1}{96}\zeta_i\eta_i^{-1}(1 - \eta^2) \\ (1 + 3\xi_0 + 3\xi^2 + 2\eta_0(2 + \xi_0)) \\ \frac{1}{8}(1 + \xi_0)(1 + \eta_0) \\ (1 + \zeta_0)(\xi_0 + \zeta_0 - 1) \end{array} \right\} \begin{array}{l} \hat{x}_i = \pm 1, \\ \hat{y}_i = \pm 1, \\ \hat{z}_i = \pm 1, \end{array}$$

$$(3.4) \quad \mathbf{N}_i^{20D}(x, y, z) = \left\{ \begin{array}{l} \left[\begin{array}{cc} 0 & -\frac{1}{24}\eta_i\xi_h^{-1}\xi(1 - \xi^2)(2 + \zeta_0) \\ 0 & \frac{1}{4}(1 - \xi^2)(1 + \eta_0)(1 + \zeta_0) \\ 0 & \frac{1}{48}\eta_i\zeta_i^{-1}(1 - \zeta^2)(5 - 3\xi^2) \end{array} \right. \\ \left. \begin{array}{cc} -\frac{1}{24}\zeta_i\xi_h^{-1}\xi(1 - \xi^2)(2 + \eta_0) \\ \frac{1}{48}\zeta_i\eta_i^{-1}(1 - \eta^2)(5 - 3\xi^2) \\ \frac{1}{4}(1 - \xi^2)(1 + \eta_0)(1 + \zeta_0) \end{array} \right] \begin{array}{l} \hat{x}_i = 0, \\ \hat{y}_i, \hat{z}_i = \pm 1, \end{array} \\ \\ \left[\begin{array}{cc} \frac{1}{4}(1 - \eta^2)(1 + \xi_0)(1 + \zeta_0) & 0 \\ -\frac{1}{24}\xi_i\eta_h^{-1}\eta(1 - \eta^2)(2 + \zeta_0) & 0 \\ \frac{1}{48}\xi_i\zeta_i^{-1}(1 - \zeta^2)(5 - 3\eta^2) & 0 \end{array} \right. \\ \left. \begin{array}{cc} \frac{1}{48}\zeta_i\xi_i^{-1}(1 - \xi^2)(5 - 3\eta^2) \\ -\frac{1}{24}\zeta_i\eta_h^{-1}\eta(1 - \eta^2)(2 + \xi_0) \\ \frac{1}{4}(1 - \eta^2)(1 + \xi_0)(1 + \zeta_0) \end{array} \right] \begin{array}{l} \hat{y}_i = 0, \\ \hat{x}_i, \hat{z}_i = \pm 1, \end{array} \\ \\ \left[\begin{array}{ccc} \frac{1}{4}(1 - \zeta^2)(1 + \xi_0)(1 + \eta_0) & \frac{1}{48}\eta_i\xi_i^{-1}(1 - \xi^2)(5 - 3\zeta^2) & 0 \\ \frac{1}{48}\xi_i\eta_i^{-1}(1 - \eta^2)(5 - 3\zeta^2) & \frac{1}{4}(1 - \zeta^2)(1 + \xi_0)(1 + \eta_0) & 0 \\ -\frac{1}{24}\xi_i\zeta_h^{-1}\zeta(1 - \zeta^2)(2 + \eta_0) & -\frac{1}{24}\eta_i\zeta_h^{-1}\zeta(1 - \zeta^2)(2 + \xi_0) & 0 \end{array} \right] \begin{array}{l} \hat{z}_i = 0, \\ \hat{x}_i, \hat{y}_i = \pm 1. \end{array} \end{array}$$

These functions are quadratic-complete over their respective fields, and display discontinuity properties similar to their linear counterparts.

4. EXTENSION TO ORTHOGONAL CURVILINEAR COORDINATES

For Lagrange interpolation of solenoidal or irrotational fields, it is not essential that the common or consistent divergence/rotation be constant. It is sufficient that the divergence/rotation of each function has a common functional form. Then there can exist a constraint among the functions such that the sum of the divergences (or curls) vanishes. In fact, the necessary and sufficient condition for zero divergence is that the net flow into each element vanishes.

As a simple example in two dimensions, consider solenoidal interpolation in polar coordinates. The choice of the form for the common or functionally-consistent divergence is not unique. For this example we will choose it to be proportional to the global variable r^{-1} . Then recalling the form of the divergence and curl

TABLE 1. Diagonal matrix \mathbf{h} for several curvilinear coordinate systems.

	Carte -sian (x, y)	Polar (r, θ)	Axisym -metric (r, z)	Spherical surface (ϑ, φ)	Cylindrical (r, ϑ, z)	Spherical (r, ϑ, φ)
\mathbf{h}	$\begin{bmatrix} 1 & 0 \\ 0 & 1 \end{bmatrix}$	$\begin{bmatrix} r^{-1} & 0 \\ 0 & 1 \end{bmatrix}$	$\begin{bmatrix} r^{-1} & 0 \\ 0 & r^{-1} \end{bmatrix}$	$\begin{bmatrix} (\sin \vartheta)^{-1} & 0 \\ 0 & 1 \end{bmatrix}$	$\begin{bmatrix} r^{-1} & 0 & 0 \\ 0 & 1 & 0 \\ 0 & 0 & r^{-1} \end{bmatrix}$	$\begin{bmatrix} (r^2 \sin \vartheta)^{-1} & 0 & 0 \\ 0 & (r \sin \vartheta)^{-1} & 0 \\ 0 & 0 & r^{-1} \end{bmatrix}$

TABLE 2. Diagonal matrix $\bar{\mathbf{h}}$ for several curvilinear coordinate systems.

	Carte -sian (x, y)	Polar (r, θ)	Axisym -metric (r, z)	Spherical surface (ϑ, φ)	Cylindrical (r, ϑ, z)	Spherical (r, ϑ, φ)
$\bar{\mathbf{h}}$	$\begin{bmatrix} 1 & 0 \\ 0 & 1 \end{bmatrix}$	$\begin{bmatrix} 1 & 0 \\ 0 & r^{-1} \end{bmatrix}$	$\begin{bmatrix} 1 & 0 \\ 0 & 1 \end{bmatrix}$	$\begin{bmatrix} 1 & 0 \\ 0 & (\sin \vartheta)^{-1} \end{bmatrix}$	$\begin{bmatrix} 1 & 0 & 0 \\ 0 & r^{-1} & 0 \\ 0 & 0 & 1 \end{bmatrix}$	$\begin{bmatrix} 1 & 0 & 0 \\ 0 & r^{-1} & 0 \\ 0 & 0 & (r \sin \vartheta)^{-1} \end{bmatrix}$

operators in polar coordinates,

$$\begin{aligned} \operatorname{div} \mathbf{V} &= r^{-1} \frac{\partial}{\partial r} r V_r + r^{-1} \frac{\partial}{\partial \theta} V_\theta, \\ \operatorname{curl} \mathbf{V} &= -r^{-1} \frac{\partial}{\partial \theta} V_r + r^{-1} \frac{\partial}{\partial r} r V_\theta, \end{aligned}$$

one finds that the (linear) common-divergence functions must be,
(4.1)

$$\mathbf{N}_i^{4D}(r, \theta) = \begin{bmatrix} \frac{1}{4}(1 + \vartheta_0)(1 + \varrho_0)(r_c + \frac{\hat{r}_i h_r}{2}) r^{-1} & \frac{1}{8} \vartheta_i \varrho_i^{-1} (1 - \varrho^2) r^{-1} \\ \frac{1}{8} \varrho_i \vartheta_i^{-1} (1 - \vartheta^2)(r_c + \frac{\hat{r}_i h_r}{2}) & \frac{1}{4}(1 + \vartheta_0)(1 + \varrho_0) \end{bmatrix} \hat{r}_i, \hat{\theta}_i = \pm 1,$$

where the local (ϱ, ϑ) and global (r, θ) coordinates are related by,

$$\begin{aligned} \varrho_i &\equiv \frac{2}{h_r}(r - r_c), & \varrho_0 &\equiv \hat{r}_i \varrho, & \varrho_h &\equiv \frac{2}{h_r}, & \varrho_i &\equiv \hat{r}_i \varrho_h, \\ \vartheta &\equiv \frac{2}{h_\theta}(\theta - \theta_c), & \vartheta_0 &\equiv \hat{\theta}_i \vartheta, & \vartheta_h &\equiv \frac{2}{h_\theta}, & \vartheta_i &\equiv \hat{\theta}_i \vartheta_h. \end{aligned}$$

Note that the global variable associated with the singular point of the coordinate system can be factored out as,

$$(4.2) \quad \mathbf{N}_i^D(r, \theta) = \mathbf{h} \bar{\mathbf{N}}_i^D(r, \theta) \mathbf{h}_i^{-1} = \begin{bmatrix} r^{-1} & 0 \\ 0 & 1 \end{bmatrix} \begin{bmatrix} \frac{1}{4}(1 + \vartheta_0)(1 + \varrho_0) & \frac{1}{8} \vartheta_i \varrho_i^{-1} (1 - \varrho^2) \\ \frac{1}{8} \varrho_i \vartheta_i^{-1} (1 - \vartheta^2) & \frac{1}{4}(1 + \vartheta_0)(1 + \varrho_0) \end{bmatrix} \begin{bmatrix} (r_c + \frac{\hat{r}_i h_r}{2}) & 0 \\ 0 & 1 \end{bmatrix} \hat{r}_i, \hat{\theta}_i = \pm 1,$$

where the subscript i on the diagonal post-multiplying matrix \mathbf{h} indicates evaluation at the node i . This factorization is not unique to polar coordinates. In fact, \mathbf{h} is given in Table 1 for a number of common coordinate systems.

A similar factorization, with different diagonal matrices denoted by $\bar{\mathbf{h}}$, can be found for the common-curl functions, and some are given in Table 2.

These are the principal results sought in this section, but a few other remarks are in order. It would seem that the interpolation function blows up at the singular points of the curvilinear coordinate systems due to terms in the matrix \mathbf{h} ($\bar{\mathbf{h}}$). In

fact, the matrix \mathbf{h}_i^{-1} ($\bar{\mathbf{h}}_i^{-1}$) has corresponding terms that vanish at nodes associated with the singular points. Consequently, some terms drop out of the unisolvence set. For the coordinate systems given above, unisolvence can be restored by adding appropriate singular terms. In a number of cases interpolation can be extended to the (singular) point at infinity. The degrees-of-freedom associated with the singularities are not the field components (which are infinite at the singular node) but rather the limit of the field component times the coordinate as the coordinate approaches the singular point (e.g. $\lim_{r \rightarrow 0} r V_r(r, \vartheta)$ at the origin in polar coordinates). This particular extension would not usually be of relevance in an application such as fluid mechanics, but might be of interest in application to electromagnetics.

5. EXTENSION TO AFFINE MESHES

We now extend the above results to affine meshes. Returning to the linear CD function (2.5), the geometric terms can be factored out as,

$$(5.1) \quad \mathbf{N}_i^{4D}(\xi, \eta) = \begin{bmatrix} \xi_h^{-1} & 0 \\ 0 & \eta_h^{-1} \end{bmatrix} \begin{bmatrix} \frac{1}{4}(1 + \xi_0)(1 + \eta_0) & \frac{1}{8}\hat{\eta}_i\hat{\xi}_i^{-1}(1 - \xi^2) \\ \frac{1}{8}\hat{\xi}_i\hat{\eta}_i^{-1}(1 - \eta^2) & \frac{1}{4}(1 + \xi_0)(1 + \eta_0) \end{bmatrix} \begin{bmatrix} \xi_h & 0 \\ 0 & \eta_h \end{bmatrix},$$

where the indices $\hat{\xi}_i, \hat{\eta}_i = \pm 1$.

The pre- and post-multiplying matrices can be recognized as related to the Jacobian matrix of the transformation from local coordinates on $[-1, 1]^2$ to the element centered at (x_c, y_c) with dimensions h_x, h_y by using the chain rule for derivatives. We write the Jacobian as,

$$(5.2) \quad \mathbf{J} = \begin{bmatrix} x, \xi & y, \xi \\ x, \eta & y, \eta \end{bmatrix}, \quad \text{or} \quad \mathbf{J} = \begin{bmatrix} x, \xi & y, \xi & z, \xi \\ x, \eta & y, \eta & z, \eta \\ x, \zeta & y, \zeta & z, \zeta \end{bmatrix},$$

where the comma notation indicates differentiation with respect to the following variable. It can be verified that the pre-multiplying matrix in (5.1) is then $\Delta^{-1}\mathbf{J}^T$, where Δ is the determinant of \mathbf{J} , and the post-multiplying matrix is the inverse of this product evaluated at the node i .

With this association, excluding nodes at the singular points of the coordinate systems, the general form of the two- or three-dimensional common-divergence interpolation functions is,

$$(5.3) \quad \mathbf{N}_i^{nD}(x, y, z) = \Delta^{-1}\mathbf{h} \mathbf{J}^T \hat{\mathbf{N}}_i^{nD}(T(\xi, \eta, \zeta))\Delta_i(\mathbf{J}_i^T)^{-1}\mathbf{h}_i^{-1},$$

where $T(\xi, \eta, \zeta)$ is the transformation to the global coordinates, and $\hat{\mathbf{N}}_i^{nD}$ is the n -node constant-divergence Cartesian interpolation function on the domain $[-1, 1]^m$, $m = 2$ or 3 . Furthermore, the integrals of the divergence of the functions are,

$$(5.4) \quad \int_{\Omega^e} \nabla \cdot \mathbf{N}_i^{4D} d\Omega = [\hat{x}_i, \hat{y}_i] \Delta_i (\mathbf{J}_i^T)^{-1} \mathbf{h}_i^{-1}, \quad \hat{x}_i = \pm 1, \hat{y}_i = \pm 1,$$

$$\int_{\Omega^e} \nabla \cdot \mathbf{N}_i^{8D} d\Omega = \begin{cases} \frac{1}{3}[\hat{x}_i, \hat{y}_i] \Delta_i (\mathbf{J}_i^T)^{-1} \mathbf{h}_i^{-1}, & \hat{x}_i = \pm 1, \hat{y}_i = \pm 1, \\ \frac{4}{3}[\hat{x}_i, 0] \Delta_i (\mathbf{J}_i^T)^{-1} \mathbf{h}_i^{-1}, & \hat{x}_i = \pm 1, \hat{y}_i = 0, \\ \frac{4}{3}[0, \hat{y}_i] \Delta_i (\mathbf{J}_i^T)^{-1} \mathbf{h}_i^{-1}, & \hat{x}_i = 0, \hat{y}_i = \pm 1. \end{cases}$$

and

$$(5.5) \quad \int_{\Omega^e} \nabla \cdot \mathbf{N}_i^{8D} d\Omega = [\hat{x}_i, \hat{y}_i, \hat{z}_i] \Delta_i (\mathbf{J}_i^T)^{-1} \mathbf{h}_i^{-1}, \quad \hat{x}_i = \pm 1, \hat{y}_i = \pm 1, \hat{z}_i = \pm 1,$$

$$\int_{\Omega^e} \nabla \cdot \mathbf{N}_i^{20D} d\Omega = \begin{cases} -\frac{1}{3}[\hat{x}_i, \hat{y}_i, \hat{z}_i] \Delta_i (\mathbf{J}_i^T)^{-1} \mathbf{h}_i^{-1}, & \hat{x}_i = \pm 1, \hat{y}_i = \pm 1, \hat{z}_i = \pm 1, \\ \frac{4}{3}[0, \hat{y}_i, \hat{z}_i] \Delta_i (\mathbf{J}_i^T)^{-1} \mathbf{h}_i^{-1}, & \hat{x}_i = 0, \hat{y}_i = \pm 1, \hat{z}_i = \pm 1, \\ \frac{4}{3}[\hat{x}_i, 0, \hat{z}_i] \Delta_i (\mathbf{J}_i^T)^{-1} \mathbf{h}_i^{-1}, & \hat{x}_i = \pm 1, \hat{y}_i = 0, \hat{z}_i = \pm 1, \\ \frac{4}{3}[\hat{x}_i, \hat{y}_i, 0] \Delta_i (\mathbf{J}_i^T)^{-1} \mathbf{h}_i^{-1}, & \hat{x}_i = \pm 1, \hat{y}_i = \pm 1, \hat{z}_i = 0. \end{cases}$$

The generalized CC function corresponding to (5.3) is

$$(5.6) \quad \mathbf{N}_i^{nC}(x, y) = \bar{\mathbf{h}} \mathbf{J}^{-1} \tilde{\mathbf{N}}_i^{nC}(T(\xi, \eta)) \mathbf{J}_i \bar{\mathbf{h}}_i^{-1},$$

where the tilde ($\tilde{}$) indicates the matrix transpose. This form is, of course, limited to two dimensions. The integral of the curl is given by,

$$(5.7) \quad \int_{\Omega^e} \nabla \times \mathbf{N}_i^{4C} d\Omega = \frac{1}{4}[\hat{y}_i, -\hat{x}_i] \mathbf{J}_i \bar{\mathbf{h}}_i^{-1}, \quad \hat{x}_i = \pm 1, \hat{y}_i = \pm 1,$$

$$\int_{\Omega^e} \nabla \times \mathbf{N}_i^{8C} d\Omega = \begin{cases} \frac{1}{12}[\hat{y}_i, -\hat{x}_i] \mathbf{J} \bar{\mathbf{h}}_i^{-1}, & \hat{x}_i = \pm 1, \hat{y}_i = \pm 1, \\ \frac{1}{3}[\hat{y}_i, 0] \mathbf{J} \bar{\mathbf{h}}_i^{-1}, & \hat{x}_i = \pm 1, \hat{y}_i = 0, \\ \frac{1}{3}[0, -\hat{x}_i] \mathbf{J} \bar{\mathbf{h}}_i^{-1}, & \hat{x}_i = 0, \hat{y}_i = \pm 1. \end{cases}$$

Remarkably, the generalizations to affine meshes (where the Jacobian matrix is constant over each element) preserve the appropriate continuity and normalization, and the interpolation functions retain their respective linear and quadratic exactness over the respective solenoidal or irrotational vector fields. But for practical purposes, the mesh need not be affine, i.e. the Jacobian matrix of the transformation need not be constant, leading to rational functions rather than polynomials. The error in such non-affine transformations has not been studied by the author, but often, particularly where the mesh has been refined, the individual elements on the non-affine mesh are sufficiently close to affine shape that the expressions above are good approximations. Of course one need not use the affine approximation, in which case the Jacobian matrices and determinants are functions of the coordinates.

6. EQUATION OF MOTION FOR INCOMPRESSIBLE FLOW

The classical form of the incompressible Navier-Stokes equation (INSE), generally recognized as describing the motion of incompressible flow in a domain Ω , is given by,

$$(6.1) \quad \frac{\partial}{\partial t} \mathbf{u} = -\mathbf{u} \cdot \nabla \mathbf{u} - \nabla p + \nu \nabla^2 \mathbf{u} + \mathbf{f},$$

$$\nabla \cdot \mathbf{u} = 0,$$

where \mathbf{u} is the fluid velocity, p is the reduced pressure, ν is the kinematic viscosity and \mathbf{f} is the body force. It appears to be a dynamic equation, but this interpretation is open to question. The nature of the equation needs to be clarified as misconceptions abound, which lead to improper application of the discrete computable form.

Under suitable boundary conditions, a vector space may be orthogonally decomposed (Helmholtz decomposition) into the sum of solenoidal and irrotational parts. This can be realized through the linear projection operators π^I and π^S , given formally by [4],

$$(6.2) \quad \pi^I = \nabla \Delta^{-1} \nabla \cdot, \quad \pi^S = 1 - \pi^I,$$

where the operator Δ^{-1} (the inverse Laplacian) is the Green's function for the Laplace equation on Ω . Applied to (6.1), this gives the pair of integro-differential equations,

$$(6.3) \quad \begin{aligned} \frac{\partial}{\partial t} \mathbf{u} &= \pi^S (-\mathbf{u} \cdot \nabla \mathbf{u} + \nu \nabla^2 \mathbf{u}) + \mathbf{f}^S, & \mathbf{u} \cdot \mathbf{n} \Big|_{\partial \Omega} &= 0, \\ \nabla p &= \pi^I (-\mathbf{u} \cdot \nabla \mathbf{u} + \nu \nabla^2 \mathbf{u}) + \mathbf{f}^I, \end{aligned}$$

with \mathbf{f}^S and \mathbf{f}^I the non-conservative (solenoidal) and conservative (irrotational) parts of the body force, respectively.

Thus it would seem that the first equation, governing the motion of the incompressible fluid, depends only on the nonconservative part of the force and does not depend on the pressure. Likewise, the pressure is a functional of the irrotational part of the fluid flow and any conservative forces. This decomposition has been recognized for a long time [2][7][8][11], but seems to have been dismissed as a “mathematical trick” [3].

The appearance of a pressure term in the equation of motion arose from an incorrect application of first principles in its derivation. In that derivation, one applied Newton's second law to a small volume of fluid. It was assumed that one force on the fluid volume resulted from a dynamic pressure difference across opposite faces of the volume, leading to a pressure gradient term. But pressure disturbances propagate at infinite speed in an incompressible medium, so no *dynamic* pressure differences can exist for a finite time, and no term of this type can appear in the *equation of motion* of the fluid.

Thus the INSE is not the dynamic equation of motion it seems to be, but is rather the sum of a kinematic equation for the fluid flow, where incompressibility plays the role of a conservation law, and an algebraic equation (in time) for the *consistent* pressure, which is a function of that flow. This distinction is important because it bears on the way the computational algorithm for the solution of the incompressible flow will be implemented. The attractiveness of the INSE is that it reduces the two integro-differential equations to a single differential algebraic equation.

The pressure in the problem domain and on the boundary is an explicit function of the velocity. However, if pressure boundary conditions are specified so that the inverse problem is well-posed, the explicit dependence of the pressure on the velocity can be inverted. Then the pair of equations (6.3) can be solved simultaneously to find the velocity as an implicit function of the pressure gradient and its boundary conditions.

7. THE PROJECTION METHOD

We start with the (pressureless) equation of motion for an incompressible fluid,

$$(7.1) \quad \frac{\partial}{\partial t} \mathbf{u} = \pi^S (-\mathbf{u} \cdot \nabla \mathbf{u} + \nu \nabla^2 \mathbf{u}) + \mathbf{f}^S \quad \text{in } \Omega.$$

Using $\pi^S = 1 - \pi^I$, this can be written as,

$$(7.2) \quad \frac{\partial}{\partial t} \mathbf{u} = -\mathbf{u} \cdot \nabla \mathbf{u} + \nu \nabla^2 \mathbf{u} + \mathbf{f}^S - \pi^I(-\mathbf{u} \cdot \nabla \mathbf{u} + \nu \nabla^2 \mathbf{u}) \quad \text{in } \Omega.$$

Since the last term is clearly irrotational, it can be written as the gradient of a scalar projection function φ . With this substitution we have the mixed equations,

$$(7.3) \quad \begin{aligned} \frac{\partial}{\partial t} \mathbf{u} &= -\mathbf{u} \cdot \nabla \mathbf{u} + \nu \nabla^2 \mathbf{u} - \nabla \varphi + \mathbf{f}^S, \\ \nabla \varphi &= \pi^I(-\mathbf{u} \cdot \nabla \mathbf{u} + \nu \nabla^2 \mathbf{u}). \end{aligned}$$

Alternatively, one can introduce the projection function as a Lagrange multiplier for the solenoidal constraint, yielding the pair of equations with φ defined implicitly,

$$(7.4) \quad \begin{aligned} \frac{\partial}{\partial t} \mathbf{u} &= -\mathbf{u} \cdot \nabla \mathbf{u} + \nu \nabla^2 \mathbf{u} - \nabla \varphi + \mathbf{f}^S, \\ \nabla \cdot \mathbf{u} &= 0. \end{aligned}$$

It looks like we have reintroduced the pressure, and this appearance is the source of a great deal of confusion. But not everything that looks like a pressure is a pressure. The projection function φ does not obey the boundary conditions of a pressure, and it does not behave like a pressure (except that it is irrotational), and there is a restriction on φ (the LBB condition) that does not apply to pressures.

To continue, we introduce equivalent weak forms of (7.3) and (7.4), obtained by multiplying by any function in an appropriate space of weight or test functions, and integrating over the problem domain. After integration by parts, the results are,

$$(7.5) \quad \begin{aligned} (\mathbf{v}, \frac{\partial}{\partial t} \mathbf{u}) &= -(\mathbf{v}, \mathbf{u} \cdot \nabla \mathbf{u}) - \nu(\nabla \mathbf{v}, \nabla \mathbf{u}) - (\mathbf{v}, \nabla \varphi) + (\mathbf{v}, \mathbf{f}^S), \\ \mathbf{u} &\in \mathbf{H}_0^1, \varphi \in H^1/0, \forall \mathbf{v} \in \mathbf{H}_0^1, \\ (\nabla q, \nabla \varphi) &= -(\nabla q, \mathbf{u} \cdot \nabla \mathbf{u}) + \nu(\nabla q, \nabla^2 \mathbf{u}), \quad \mathbf{u} \in \mathbf{H}_0^1, \varphi \in H^1/0, \forall q \in H^1/0, \end{aligned}$$

and,

$$(7.6) \quad \begin{aligned} (\mathbf{v}, \frac{\partial}{\partial t} \mathbf{u}) &= -(\mathbf{v}, \mathbf{u} \cdot \nabla \mathbf{u}) - \nu(\nabla \mathbf{v}, \nabla \mathbf{u}) + (\nabla \cdot \mathbf{v}, \varphi) + (\mathbf{v}, \mathbf{f}^S), \\ \mathbf{u} &\in \mathbf{H}_0^1, \varphi \in L_0^2, \forall \mathbf{v} \in \mathbf{H}_0^1, \\ (q, \nabla \cdot \mathbf{u}) &= 0, \quad \mathbf{u} \in \mathbf{H}_0^1, \forall q \in L_0^2, \end{aligned}$$

where (\cdot, \cdot) indicates the inner product over Ω . The remaining projection operator in the first pair (7.3) disappears; the projection is accomplished by the orthogonality of the gradient of the projection space. The first pair of equations can be recognized as a ‘‘pressure projection’’ method [4].

Since the purpose of φ is to project out the irrotational part of (7.3–7.6), not any space for φ will do; it is intimately related to the space of \mathbf{u} . This relation is expressed by the Ladyzhenskaya-Babuska-Brezzi (LBB) or inf-sup condition [2][11] on Ω ,

$$(7.7) \quad \inf_{0 \neq q \in Q} \sup_{0 \neq \mathbf{v} \in \mathbf{V}} \frac{(\mathbf{v}, \nabla q)}{\|\mathbf{v}\|_1 \|q\|_0} \geq \gamma > 0, \quad \mathbf{v} \in \mathbf{V} \subset \mathbf{H}_0^1, \quad q \in Q \subset L_0^2.$$

Satisfaction of this condition assures that (7.3–7.6) are well-posed.

When the velocity of the fluid is found, the pressure is recovered by

$$(7.8) \quad \begin{aligned} (\nabla q, \nabla p) &= -(\nabla q, \mathbf{u} \cdot \nabla \mathbf{u}) + \nu(\nabla q, \nabla^2 \mathbf{u}) + (\nabla q, \mathbf{f}^I), \\ p &\in \mathbf{H}^1/0, \mathbf{u} \in \mathcal{V}, \forall q \in \mathbf{H}^1/0, \mathcal{V} = \{v \in \mathbf{H}_0^1 : \nabla \cdot v = 0\}, \end{aligned}$$

There is no LBB restriction on the approximation space for p because \mathbf{u} is divergence-free here, so this is a pressure, not a projection.

8. THE ALGEBRAIC PROBLEM

Let the problem domain Ω be partitioned into non-overlapping affine quadrilateral or hexahedral subdomains Ω^e with h a measure of the diameter of these subdomains, and such that $\Omega^h = \cup_e \Omega^e$. For convenience, assume homogeneous Dirichlet boundary conditions. Let $\mathbf{V}^h \in \mathbf{H}(\text{div}, \Omega^h)$ be the space spanned by the set of functions $\{\mathbf{N}_i^D\}$ introduced earlier, and \mathbf{V}_0^h the subspace of such functions that vanish on the boundary $\partial\Omega^h$. Let the degrees-of-freedom at each node of the mesh be the vector components of the flow field \mathbf{u}^h at the node. Since the divergence error in the flow field is piecewise-constant, it seems appropriate to choose a basis Φ^h for φ that is piecewise-constant. The appropriate governing equation will be the discrete form of (7.6) in Ω^h ,

$$(8.1) \quad \begin{aligned} (\mathbf{v}^h, \frac{\partial}{\partial t} \mathbf{u}^h) &= -(\mathbf{v}^h, \mathbf{u}^h \cdot \nabla \mathbf{u}^h) - \nu(\nabla \mathbf{v}^h, \nabla \mathbf{u}^h) \\ &\quad + (\nabla \cdot \mathbf{v}^h, \varphi^h) + (\mathbf{v}^h, \mathbf{f}^S), \quad \mathbf{u}^h \in \mathbf{V}_0^h, \forall \mathbf{v}^h \in \mathbf{V}_0^h, \\ (\phi^h, \nabla \cdot \mathbf{u}^h) &= 0, \quad \mathbf{u}^h \in \mathbf{V}_0^h, \varphi^h \in \Phi^h, \forall \phi^h \in \Phi^h, \end{aligned}$$

and for the pressure,

$$(8.2) \quad \begin{aligned} (\nabla q^h, \nabla p^h) &= -(\nabla q^h, \mathbf{u}^h \cdot \nabla \mathbf{u}^h) + \nu(\nabla q^h, \nabla^2 \mathbf{u}^h) + (\nabla q^h, \mathbf{f}^I), \\ p^h &\in \mathbf{H}^1, \mathbf{u}^h \in \mathcal{V}, \forall q^h \in \mathbf{H}^1, \mathcal{V} = \{v \in \mathbf{H}^1 : \nabla \cdot v = 0\} \end{aligned}$$

Taking the test and trial functions for the velocity to be $\{\mathbf{N}_i^D\}$, and using the set of bilinear functions $\{n_i\}$ for the pressure results in the algebraic equations,

$$(8.3) \quad \begin{aligned} \mathbf{M}_{ij} u_{j,t} &= -\mathbf{C}_{ij}(\mathbf{u}^h) u_j + \nu \mathbf{D}_{ij} u_j + \mathbf{B}_{ik} \phi_k + \mathbf{F}_i, \\ \mathbf{B}_{kj} u_j &= 0, \\ \bar{\mathbf{M}}_{ij} p_j &= -\bar{\mathbf{C}}_{ij}(\mathbf{u}^h) u_j + \nu \bar{\mathbf{D}}_{ij} u_j + \bar{\mathbf{F}}_i, \end{aligned}$$

where the global matrices are assembled from,

$$(8.4) \quad \begin{aligned} \mathbf{M}_{ij}^e &= \int_{\Omega^e} \mathbf{N}_i^T \mathbf{N}_j d\Omega, & \mathbf{C}_{ij}^e(\mathbf{u}^h) &= \int_{\Omega^e} \mathbf{N}_i^T (\mathbf{u}^h \cdot \nabla) \mathbf{N}_j d\Omega, \\ \mathbf{D}_{ij}^e &= -\int_{\Omega^e} (\nabla_k \mathbf{N}_i)^T \nabla_k \mathbf{N}_j d\Omega, & \mathbf{F}_i^e &= \int_{\Omega^e} \mathbf{N}_i^T \mathbf{f}^S d\Omega, \\ \mathbf{B}_{kj}^e &= \int_{\Omega^e} \delta_{ke} \nabla \cdot \mathbf{N}_j d\Omega, \end{aligned}$$

where $\phi_k = \delta_{ke} = 1$ if k is in element e and is zero otherwise, and

$$(8.5) \quad \begin{aligned} \bar{\mathbf{M}}_{ij}^e &= \int_{\Omega^e} (\nabla \mathbf{n}_i)^T (\nabla \mathbf{n}_j) d\Omega, & \bar{\mathbf{C}}_{ij}^e(\mathbf{u}^h) &= \int_{\Omega^e} (\nabla \mathbf{n}_i)^T (\mathbf{u}^h \cdot \nabla) \mathbf{N}_j d\Omega, \\ \bar{\mathbf{D}}_{ij}^e &= \int_{\Omega^e} (\nabla \mathbf{n}_i)^T \nabla^2 \mathbf{N}_j d\Omega, & \bar{\mathbf{F}}_i^e &= \int_{\Omega^e} (\nabla \mathbf{n}_i)^T \mathbf{f}^I d\Omega. \end{aligned}$$

In the following example we assume two-dimensional Cartesian coordinates and an affine mesh. The general non-affine case would involve derivatives of the Jacobian matrix, determinants and the matrix \mathbf{h} .

Substituting the general forms of the interpolation functions and transforming to integrate over the square $[-1, 1]^2$,

$$\begin{aligned}
(8.6) \quad \mathbf{M}_{ij}^e &= \int_{-1}^1 d\xi \int_{-1}^1 d\eta \Delta \left((\Delta^{-1} \mathbf{J}^T \hat{\mathbf{N}}_i(\xi, \eta) \Delta_i(\mathbf{J}_i^T)^{-1})^T \Delta^{-1} \mathbf{J}^T \hat{\mathbf{N}}_j(\xi, \eta) \Delta_j(\mathbf{J}_j^T)^{-1} \right), \\
\mathbf{C}_{ij}^e(\mathbf{U}) &= \int_{-1}^1 d\xi \int_{-1}^1 d\eta \Delta \left(\Delta^{-1} \mathbf{J}^T \hat{\mathbf{N}}_i(\xi, \eta) \Delta_i(\mathbf{J}_i^T)^{-1} \right)^T \\
&\quad \{ U_0 \hat{\mathbf{N}}_{j,x}(\xi, \eta) + V_0 \hat{\mathbf{N}}_{j,y}(\xi, \eta) \}, \\
\mathbf{D}_{ij}^e &= - \int_{-1}^1 d\xi \int_{-1}^1 d\eta \Delta \left(\mathbf{N}_{i,x}^T(\xi, \eta) \mathbf{N}_{j,x}(\xi, \eta) + \mathbf{N}_{i,y}^T(\xi, \eta) \mathbf{N}_{j,y}(\xi, \eta) \right), \\
\mathbf{F}_i^e &= \int_{-1}^1 d\xi \int_{-1}^1 d\eta \Delta \left((\Delta^{-1} \mathbf{J}^T \hat{\mathbf{N}}_i(\xi, \eta) \Delta_i(\mathbf{J}_i^T)^{-1})^T \mathbf{f}^S \right),
\end{aligned}$$

where,

$$\begin{aligned}
(8.7) \quad \mathbf{N}_{k,x}(\xi, \eta) &= \Delta^{-1} \mathbf{J}^T (J_{11}^{-1} \hat{\mathbf{N}}_{k,\xi}(\xi, \eta) + J_{21}^{-1} \hat{\mathbf{N}}_{k,\eta}(\xi, \eta)) \Delta_k(\mathbf{J}_k^T)^{-1} \\
\mathbf{N}_{k,y}(\xi, \eta) &= \Delta^{-1} \mathbf{J}^T (J_{12}^{-1} \hat{\mathbf{N}}_{k,\xi}(\xi, \eta) + J_{22}^{-1} \hat{\mathbf{N}}_{k,\eta}(\xi, \eta)) \Delta_k(\mathbf{J}_k^T)^{-1} \quad k = i, j.
\end{aligned}$$

The element matrix \mathbf{B}_{ij}^e is given by one of the forms (5.4). For the four-node linear elements (2.4),

$$(8.8) \quad \mathbf{B}_{ij}^e = [\hat{x}_i, \hat{y}_i] \Delta_i(\mathbf{J}_i^T)^{-1}.$$

These terms are easily evaluated for global assembly if a structured mesh is generated with the coordinates and Jacobian matrix given at given each nodal point. For more complicated geometries, block-structured meshes can be used. Use on unstructured meshes is not precluded, though it does require substantially more data in this case. Meshing is discussed further in [6] where more powerful tools are introduced.

The quadratic velocity-piecewise constant projection function pairs satisfy the LBB condition. The linear-velocity piecewise-constant function pairs do not satisfy the LBB condition (7.7) on a structured completely rectangular mesh (but they do satisfy it on each of the ‘‘red’’ and ‘‘black’’ subdomains described below). Other than the usual ‘‘hydrostatic’’ mode, this pair possesses only the checkerboard mode on such a mesh. This mode can be removed by altering the connectivity of the mesh to destroy the checkerboard symmetry as shown later, but in practice this is of no consequence by the following heuristic argument.

Consider a square domain with homogeneous Dirichlet boundary conditions, which has been partitioned by a square mesh. Label the squares by the colors red and black, like a checkerboard. For any given internal square, immediately adjacent squares have different colors, while diagonally-adjacent squares have the same color. Resolve the flow into diagonal components. Suppose the flow in each element is determined by the four corner nodes. Observe that diagonal flow carries fluid from a square of one color into a square of the same color by flow through the common adjacent squares of the opposite color. Because the flow is diagonal, there is as much fluid flowing out of these adjacent squares as flows in; diagonal flow does not affect the net inflow in the adjacent squares.

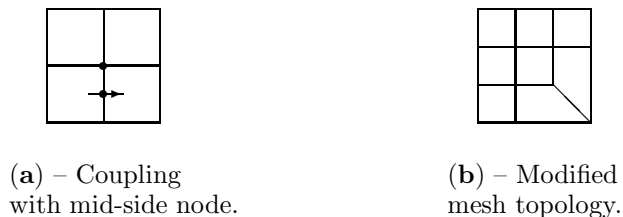
Starting in a corner with one color, adjust the magnitude of the flow at the internal node so that the net flow in/out is zero. Proceed to an appropriate node of the second square of the same color and repeat the process. If the order of adjustment is chosen properly, one eventually arrives at the last remaining square of the selected color. The net flow into that square will already be zero by the homogeneous boundary condition on the flow, so this represents a redundant constraint. One repeats the process with the squares of the opposite color, eventually leading to a second redundant constraint.

Thus, on a mesh with this kind of connectivity and using four-node Lagrange interpolation functions, there are two redundant continuity constraints. This redundancy can be eliminated by assigning arbitrary values to the projection function on one element of each color. In general, this will result in a recognizable checkerboard pattern in the projection function values. But the projection function is not a physical property like the pressure, so there is no a priori reason for excluding the checkerboard mode, and it does not affect the resulting velocities.

A similar result was deduced by Sani et. al. [10]. However, their arguments are clouded by their failure to resolve the distinction between the projection functions and the pressure detailed in Section 7.

Of course the checkerboard topology can be avoided by introducing at least one midside node with a normal-flow degree-of-freedom, which couples the two checkerboard domains as shown in Figure 1a, or by modifying the mesh at some point as shown in Figure 1b.

FIGURE 1



In principle one could ignore the constraint redundancies and solve the system of equations using a method such as the pseudo inverse, but this is not really practical for many problems of interest.

9. APPLICATION TO COUETTE-TAYLOR FLOW

Now consider the application to a Stokes problem, stationary Couette-Taylor flow. The region between two long, concentric, differentially-rotating cylinders is filled with a viscid fluid. Away from the ends of the cylinder, the flow is circumferential and can be treated as a two-dimensional problem.

The problem domain between the cylinders is discretized by a curved Cartesian mesh, with the coordinates and Jacobian matrix of the geometric transformation given at each node. The inner cylinder radius is two units and the outer radius is four units. The inner cylinder in this instance is taken to be stationary, with the outer cylinder rotating with a unit angular velocity. No-slip conditions are assumed

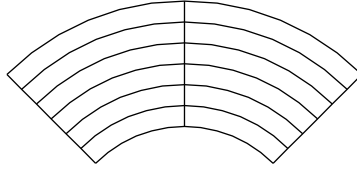
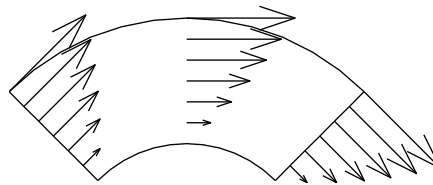
FIGURE 2. 3×7 Couette-Taylor mesh.

FIGURE 3. Couette-Taylor flow field at the nodes.

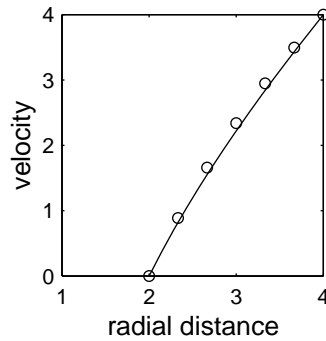


FIGURE 4. Couette-Taylor velocity profile comparison.

at the cylinder surfaces. The governing equation used is the weak Lagrangian multiplier form (8.1) and the resulting algebraic form (8.3) et. seq., with the convection, acceleration and body force terms omitted.

The problem was coded in Matlab, using the sparse matrix representation and the GMRES iterative solver with an incomplete LU preconditioner. The two redundant continuity constraints were removed by setting the projection function φ to zero on two adjacent elements. One quarter of the total domain was simulated using the 3×7 node curved mesh shown in Figure 2. The affine approximation was used. No boundary conditions were applied at the inlet and outlet boundaries where the flow is considered to be fully developed. The resulting vector flow field at the nodes is plotted in Figure 3. The computed circumferential velocities at the nodes in the center of the mesh are plotted as circles in Figure 4, and compared with the analytical solution shown as the solid curve. The L^∞ norm of the divergence error was $\|\tilde{\mathbf{B}}\mathbf{u}\|_{L^\infty} \sim 10^{-15}$.

This is not a particularly challenging problem. It was chosen simply to illustrate the removal of the dual constraint redundancies, and the use of a curved mesh with long, thin, bent, nonaffine elements, as the latter seem to present difficulties with other methods.

10. CONCLUDING REMARKS

As remarked earlier, all the interpolation functions/elements presented here display potential quadratic or cubic tangential or slip discontinuities between the nodes. This lack of control at boundaries seems (almost) unavoidable. But this may not be perceived as the difficulty it once was. Indeed, the development and study of discontinuous functions, where the *normal* component of flow is only weakly continuous, seems popular now. In fact, the potential for development of discontinuities increases the compliance of the interpolation, and so may suppress to some extent, or delay the onset of oscillations. Nevertheless, the bias toward continuity may have hindered the discovery of methods such as described here, as will be discussed later.

The unisolvence sets of the functions are linearly or quadratically exact and remain so under affine transformations, and remain complete under general invertible transformations. This exactness has been verified by enumeration using a symbolic mathematics program (Maple), and completeness can be shown directly[9]. Thus, if the field being interpolated is sufficiently smooth, the tangential discontinuities may not be manifest.

Suppose the field being interpolated is sufficiently smooth that at any point p , for any tolerance $\epsilon > 0$ there exists a disk (ball) of radius δ where the contribution to the Taylor expansion of the field about p from the second or third and higher order derivatives is less than ϵ so that these terms can be neglected. Then if the mesh is refined sufficiently that each adjacent pair of elements lies in some such disk (ball), then the interpolated field will be continuous within error ϵ . Consequently, with sufficient mesh refinement the slip discontinuities can be made negligible, and the presence of non-negligible discontinuities signal the need for further mesh refinement.

The above argument fails near the boundary of the problem domain, where the higher order derivatives on the boundary of the interpolated field are unlikely to vanish. But vorticity sheets on the boundary remain troubling to some, despite the fact that boundary layers are often not resolved, which allows some slippage. Because of the nonlocal character of the divergence constraint, field values at nodes off the boundary may induce nonzero tangential flow components on the boundary between the nodes. For “linear” elements the discontinuity has quadratic variation and is $O(h^2)$, while for “quadratic” elements the discontinuity is cubic and $O(h^3)$. With judiciously chosen stream function bubbles it is possible to render the tangential field component exactly zero on the boundaries of elements which are not on an internal corner, and zero on average for elements at an internal corner. It is not possible, in general, to eliminate discontinuities, rather one can shift the discontinuity from an external boundary to an internal interface. Computationally, the contribution of the bubble would be condensed out prior to assembly of the global matrix.

The following discussion is limited to the linearly-complete functions on a rectangular mesh in Cartesian coordinates. Referring to (2.4), the discontinuity at a

surface results from a variation in the direction tangential to the surface of the flow components normal to the surface at the nodes off the surface.

If the surface normal is in the x -direction, one adds the function,

$$(10.1) \quad \mathbf{N}_i^{4xb}(\xi, \eta) = \begin{bmatrix} -\frac{1}{16}\hat{\xi}_b\eta_0(1-\xi^2)(1-\hat{\xi}_b\xi_0) & 0 \\ \frac{1}{32}\xi_i\eta_i^{-1}(1-\eta^2)(1-\hat{\xi}_b\xi_0)(1+3\hat{\xi}_b\xi_0) & 0 \end{bmatrix},$$

where $\hat{\xi}_b = \pm 1$ is the x -coordinate index of the boundary edge, and i ranges over the nodes not on the boundary. Notice that this will make the quadratic discontinuity term vanish on the boundary edge, but an additional cubic discontinuity term is introduced on element boundaries adjacent to the external boundary, so this would be of no use at a corner.

If the surface normal is in the y -direction, one adds the function,

$$(10.2) \quad \mathbf{N}_i^{4yb}(\xi, \eta) = \begin{bmatrix} 0 & \frac{1}{32}\eta_i\xi_i^{-1}(1-\xi^2)(1-\hat{\eta}_b\eta_0)(1+3\hat{\eta}_b\eta_0) \\ 0 & -\frac{1}{16}\hat{\eta}_b\xi_0(1-\eta^2)(1-\hat{\eta}_b\eta_0) \end{bmatrix},$$

where $\hat{\eta}_b = \pm 1$ is the y -coordinate index of the boundary edge, and again i ranges over the nodes not on the boundary.

For convex corner elements one may add the function,

$$(10.3) \quad \mathbf{N}_i^{4cb}(\xi, \eta) = \frac{1}{32} \begin{bmatrix} -\hat{\xi}_b\hat{\eta}_b(1-\xi^2)(1-\hat{\xi}_b\xi_0) & \eta_i\xi_i^{-1}(1-\xi^2)(1-\hat{\xi}_b\xi) \\ (1-\hat{\eta}_b\eta)(1-3\hat{\eta}_b\eta_0) & (1-\hat{\eta}_b\eta)(1+3\hat{\eta}_b\eta_0) \\ \xi_i\eta_i^{-1}(1-\eta^2)(1-\hat{\eta}_b\eta_0) & -\hat{\eta}_b\hat{\xi}_b(1-\eta^2)(1-\hat{\eta}_b\eta_0) \\ (1-\hat{\xi}_b\xi_0)(1+3\hat{\xi}_b\xi_0) & (1-\hat{\xi}_b\xi_0)(1-3\hat{\xi}_b\xi_0) \end{bmatrix}.$$

Note that the discontinuities depend only on the field at the single interior corner node i . In this case a zero is introduced at the center of each boundary edge so the average discontinuity vanishes.

Bubbles have been touted as a palliative for the many ills encountered in the numerical solution of the incompressible Navier-Stokes equation, so we conclude with a bubble connection. In 1985, M. Fortin and A. Fortin [1] introduced the implicit form of a linear element with weakly-constant divergence. They added a bubble to the bilinear function (2.3), together with the condition that certain (non-constant) weighted integrals of the divergence over the element vanish. They defined the element implicitly, evaluating and post-processing the element matrix prior to assembly by subtracting appropriate combinations of the two bubble function rows and columns before discarding them, a process resembling static condensation. If one evaluates the function explicitly, one finds,

$$\mathbf{N}_i^{4D}(\xi, \eta) = \begin{bmatrix} \frac{1}{4}(1+\xi_0)(1+\eta_0) & \frac{3}{16}\eta_i\xi_i^{-1}(1-\xi^2)(1-\eta^2) \\ \frac{3}{16}\xi_i\eta_i^{-1}(1-\eta^2)(1-\xi^2) & \frac{1}{4}(1+\xi_0)(1+\eta_0) \end{bmatrix},$$

which has the form of (2.4) with no tangential discontinuity, and has constant divergence in the weak sense.

REFERENCES

1. M. Fortin and A. Fortin, "Newer and newer elements for incompressible flow," *Finite Elements in Fluids* **6**, John Wiley & Sons Ltd. (1985) 171–187.
2. V. Girault and P. -A. Raviart, *Finite Element Approximation of the Navier–Stokes Equations, Theory and algorithms*, Springer-Verlag, Berlin, 1979.

3. V. Girault, personal communication.
4. P. M. Gresho and R. L. Sani, *Incompressible Flow and the Finite Element Method*, John Wiley & Sons, Ltd., New York, 1998.
5. D. F. Griffiths, "An approximately divergence-free 9-node velocity element (with variations) for incompressible flows," *Int. J. Num. Meth. Fluids* **1**, (1981) 323–346.
6. J. T. Holdeman, "II. Some Hermite interpolation functions for solenoidal and irrotational vector fields," (Obelisk Research Report).
7. J. Leray, "Etude de diverses équations intégrales nonlinéaires et de quelques problèmes que pose l'hydrodynamique," *J. Math. Pures Appl.* **12** (1933) 1–82.
8. J. -L. Lions, *Quelques Méthodes de Résolution des Problèmes aux Limites Non Linéaires*, Dunod, Paris, 1969.
9. J. Petera, J. F. T. Pittman, "Isoparametric Hermite elements," *Int. J. Numer. Methods Engr.*, **37**, 3489-3519, 1994.
10. R. L. Sani, P. M. Gresho, R. L. Lee and D. F. Griffiths, "The cause and cure (?) of the spurious pressures generated by certain FEM solutions of the incompressible Navier-Stokes equations: part 1," *Int. J. Num. Meth. Fluids.* **1** 17–43 (1981).
11. R. Temam, *Navier–Stokes Equations, Theory and Numerical Analysis*, North-Holland Publishing Company, New York, 1977.

1056 LOVELL ROAD, KNOXVILLE, TENNESSEE 37932
E-mail address: `j.t.holdeman@charter.net`